of 68.9 MPa. It has a manually-controlled lever which is used to apply the hydraulic pressure. The compressed specimens have a height of roughly 80 mm. 5 mm each from the top and bottom parts of a specimen are trimmed to avoid any inhomogeneity at the edges of the specimen. A prepared specimen is shown in Fig. 4b. The trimmed soils were used to measure the water content of the specimens. The specimens of 70 mm in height and 35 mm in diameter were used for the triaxial compression tests. Two identical specimens of the same degree of saturation were prepared to obtain the strength parameters using the Mohr circle. Table 2 gives the basic information of the specimens. In the specimen notation (see Table 2), e.g., PS5-2, PS denotes "partially-saturated", 5 denotes confining pressure of 0.5 MPa (1 for 0.1 MPa of confining pressure) and 2 denotes simply the specimen number under the same confining pressure. In Table 2, PS1-1 and PS5-1 specimens were prepared without adding water. Therefore, the specimens contain the initial water content of bentonite (i.e., around 6.7-7.0%). PS1-6 and PS5-6 specimens were prepared with a high water content (e.g., around 20%) such that they are near the quasi-saturation state (i.e., S_r > 90%; S_r is degree of saturation). The water content and the degree of saturation given in Table 2 are the measured values, which are slightly deviated from the designed values, probably due to slightly uneven distribution of water across the sample and/or loosing of water during specimen preparations (e.g., due to evaporation, etc.).

(a) (b)

Fig. 3 (a) The high-pressure water sprayer and (b) the mold used to prepare the specimens with its manual compression tool

2.2 Testing apparatus and loading condition

Unconsolidated undrained (UU) triaxial compression tests were conducted to investigate the strength properties of sand-bentonite specimens. The UU tests were conducted to simulate the field conditions appropriately. The triaxial compression tests were conducted under 0.1 and 0.5 MPa of confining pressures to obtain the strength parameters (i.e., cohesion and internal friction angle). The specimens were covered with a 3 mm thick membrane to avoid water squeeze into it in addition to the usually applied measures. The testing set up was developed such that the confining pressure applied to the outer cell also goes into the inner cell (see Fig. 5). Therefore, the confining pressure applied to the outer cell is also applied on the specimen mounted in the inner cell.

(a) (b)

Fig. 4 (a) The hydraulic jack and (b) a prepared specimen

Table 2 The basic information of the specimens

Specimen notation	Water content, w (%)	Degree of saturation, S_r (%)	Confining pressure, σ_c (MPa)
PS1-1	6.98	29.0	0.1
PS5-1	6.71	28.1	0.5
PS1-2	10.01	41.8	0.1
PS5-2	10.33	42.9	0.5
PS1-3	11.36	49.0	0.1
PS5-3	11.24	46.4	0.5
PS1-4	14.05	62.7	0.1
PS5-4	13.13	62.4	0.5
PS1-5	16.24	76.2	0.1
PS5-5	17.08	73.3	0.5
PS1-6	21.14	86.8	0.1
PS5-6	19.60	85.9	0.5

The volume change of the specimens were also measured using the newly developed double-cell type triaxial apparatus shown in Fig. 5. The volume change of the specimen is measured by the volume change of a burette attached to the triaxial testing apparatus. The volumetric strain is evaluated using Eq. (3). The volume change of a specimen is governed by the volume change in the burette and the part of the loading rod entered into the inner cell as given in Eq. (4). The volume change in the burette is measured by a differential pressure transducer, which has a capacity of 10 kPa.

$$\varepsilon_{\mathrm{vol}} = \frac{\Delta V_{\mathrm{s}}}{V_{\mathrm{s,i}}} \times 100(\%) \tag{3}$$

Where ε_{vol} is volumetric strain, ΔV_s is the volume change of a specimen and $V_{s,i}$ the initial volume of the specimen.

$$\Delta V_{\mathrm{s}} = \Delta V_{\mathrm{b}} - V_{\mathrm{lr}} \tag{4}$$

Where ΔV_b is the volume change in the burette and V_{rl} is the volume of water replaced by the part of the loading rod (i.e., a cylindrical part with 8 mm diameter) penetrated into the inner cell.

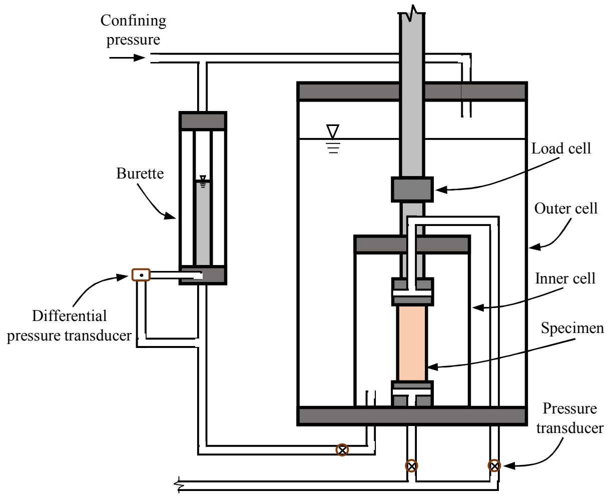

Fig. 5 Schematic diagram of the triaxial testing apparatus

The vertical load was applied with a loading rate of 0.5%/min. The shearing is conducted under undrained condition while the specimen is subjected to isotropic confining pressure. The load is applied by a Mega-torque motor. The load cell has a capacity of 10 KN. The confining pressure is applied by a pneumatic cell pressure loading system, and measured by a pressure transducer which has a capacity of 5 MPa. The loading was continued until the specimen reaches 15% of axial strain. The triaxial compression tests were performed according the Japanese standard (i.e., JGS 2009).

3. Results and Discussion

Figs. 6a and 6b show the stress-strain relationships of the specimens subjected to 0.1 and 0.5 MPa of confining pressure respectively. Fig. 6a indicates that less-saturated specimens (e.g., S_r < 63%; S_r is degree of saturation) exhibit strain-softening behaviour under a low confining pressure. That indicates a less-saturated sand-bentonite material under a small confining pressure behaves as a brittle rock, which yields a clear peak stress followed by a stress reduction. In contrast, a highly saturated sand-bentonite composite material (particularly near its quasi-saturation state) under a small confining pressure exhibits strain-hardening behaviour as a loose sand (see Fig. 6a). However, under a high confining pressure (e.g., 0.5 MPa), all the specimens except the ones under its initial moisture content of bentonite exhibit strain-hardening behaviour (see Fig. 6b). The results of stress-strain relationships also suggest a higher confining pressure yield a higher deviator stress. The results suggest that the strength properties decrease with the degree of saturation, which indicates the high strength properties of sand-bentonite composite material at the construction state weakens during the operation of a nuclear waste repository.

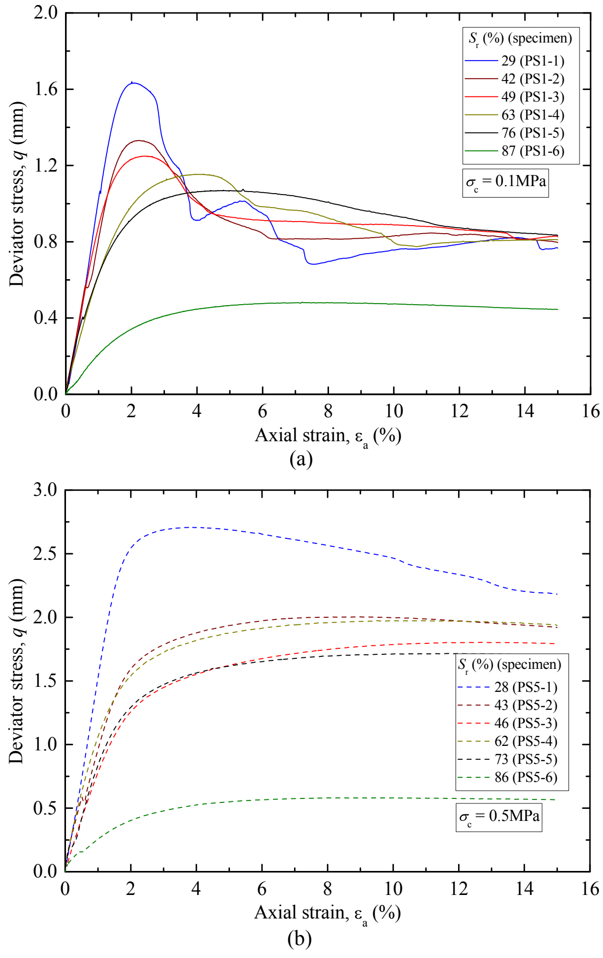

Fig. 6 Stress-strain relationships under (a) 0.1 and (b) 0.5 MPa of confining pressure respectively (S_r is degree of saturation)

Figs. 7a and 7b show the volumetric behaviour of the specimens subjected to 0.1 and 0.5 MPa of confining pressure respectively. In Figs. 7a and 7b, positive values of ε_{vol} indicate the compression behaviour while negative values of ε_{vol} indicate the expansion behaviour of the specimens. The specimens of initial moisture content of bentonite (i.e., PS1-1 and PS5-1 specimens) exhibit compression in pre-failure state followed by expansion in post-failure state independently of the confining pressure. As shown in Fig. 7a, the specimens start to yield less expansion in post-failure state with increasing degree of saturation under a small confining pressure (i.e., 0.1 MPa). As shown in Fig. 7b, under a high confining pressure (i.e., 0.5 MPa), all the specimens apart from the specimen of the initial moisture content (of bentonite) exhibit compression behaviour. It was also observed that the specimens of high water contents (i.e., except PS5-1 and PS5-2 specimens) continue to exhibit compression in post-failure state too. The compression decreases with the degree of saturation. The results hence suggest that a sand-bentonite buffer material reduces its volumetric expansion in residual strength state with time under a small confining pressure (assuming that the buffer material is subjected to continuous water flow during its operation).

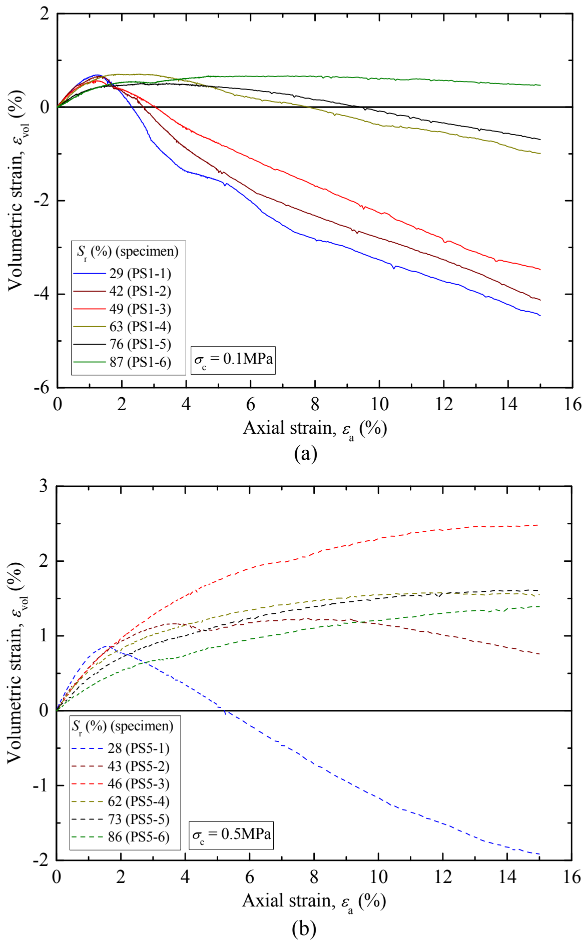

Fig. 7 Volumetric behaviour of the specimens under (a) 0.1 and (b) 0.5 MPa of confining pressure respectively (S_r is degree of saturation)

Fig. 8 shows a typical Mohr circle and its failure envelope. In case of the specimens with strain-hardening behaviour, the maximum stresses (i.e., axial and lateral stresses) either at the end of the testing (i.e., ε_a = 15%; ε_a is axial strain) or near it were considered to draw the Mohr stress circles. Fig. 9 shows the variation of strength parameters of the specimens with the degree of saturation. The degree of saturation given in Fig. 9 is the average of the two identical specimens tested under 0.1 and 0.5 MPa of confining pressure. The results indicate that, on average both cohesion and friction angle reduce with the degree of saturation. However, undrained cohesion remains unchanged during early saturation (i.e., up to 48% of S_r; S_r is degree of saturation). In contrast, undrained friction angle decreases with the early saturation, and then indicates a slight increase at 62% of S_r followed by continuous reduction. The results of friction angle indicates that a high as 35 degree friction angle of sand-bentonite buffer material at the construction state reduces to low as 6 degree at the quasi-saturation state. In comparison, the reduction of cohesion of the buffer material is not as high as friction angle since it reduces only from 0.36 MPa to 0.20 MPa from the construction state to quasi-saturation state (see Fig. 9). In a previous study, Cho et al. (2002) also reported that unconfined compressive strength of Kungel-VI bentonite decreases with water content, which agrees well with the findings of this study.

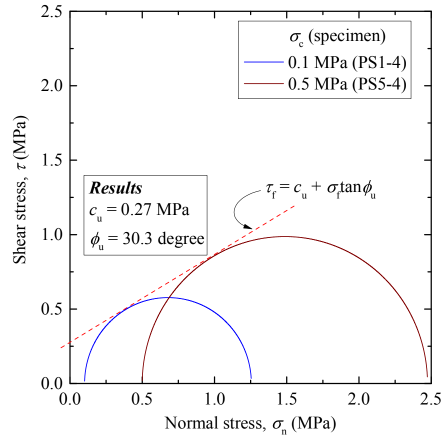

Fig. 8 A typical Mohr circle and its failure envelope (S_r = 62.6%; S_r is degree of saturation and σ_c is confining pressure)

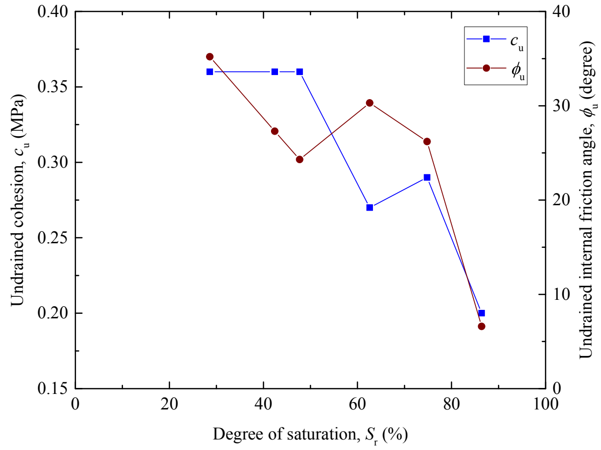

Fig. 9 The variation of undrained cohesion and internal friction angle with the degree of saturation

4. Conclusions

The strength and volume change behaviour of sand-bentonite buffer material of nuclear waste repositories were investigated by unconsolidated undrained (UU) triaxial compression tests. The specimens were prepared with various degree of saturation to understand the behaviour of buffer materials after the operation of a nuclear waste facility. The following conclusions were drawn from the study.

The specimens exhibit strain-softening behaviour under a small confining pressure (i.e., 0.1 MPa), particularly when they are still in the early saturation (e.g., roughly 50% < S_r; S_r is degree of saturation). When the degree of saturation becomes higher, the specimens start to show strain-hardening behaviour. In contrast, all the specimens apart from the one with its initial moisture content (of bentonite) under a high confining pressure (i.e., 0.5 MPa) exhibit strain-hardening behaviour. The specimens with a higher confining pressure also give higher stresses.

It was also found that the specimens except the ones with initial moisture content (of bentonite) exhibit continuous compression behaviour (both in pre- and post-failure states) under a high confining pressure (i.e., 0.5 MPa). In contrast, the specimens under a small confining pressure (i.e., 0.1 MPa) yield expansion in post-failure state after exhibiting compression in pre-failure state. The magnitude of the final expansive strain is greatly influenced by the degree of saturation, with the natural sand-bentonite specimen (i.e., which has the initial moisture content of bentonite) yielding the maximum values while the specimen near to its quasi-saturation state showing the smallest value.

The strength properties are influenced largely by the degree of saturation, particularly when the specimens near the quasi-saturation state. The undrained friction angle decreases with the degree of saturation, particularly indicating noticeable reduction near the quasi-saturation state. The undrained cohesion remains unchanged at early saturation, then start to decrease with the degree of saturation. It was also observed that the confined compressive strength increases with the confining pressure.

Reference

1. Agus, S.S., Schanz, T. and Fredlund, D.G.: Measurements of suction versus water content for bentonite-sand mixtures, Canadian Geotechnical Journal, Vol. 47, No. 5, pp. 583-594, 2010.
2. Cho, W.-J., Lee, J.-O. and Kang, C.-H.: A compilation and evaluation of thermal and mechanical properties of bentonite-based buffer materials for a high level waste repository, Journal of the Korean Nuclear Society, Vol. 34, No. 1, pp. 90-103, 2002.
3. JGS 0521: Method for unconsolidated-undrained triaxial compression test on soils, Japanese Geotechnical Society (JGS) Standard, Tokyo, Japan, 2009.
4. Kodaka, T. and Teramoto, Y.: Shear failure behavior of compacted bentonite, Proc. International Symposium on Prediction and Simulation Methods for Geohazard Mitigation, Kyoto, Japan, pp. 331-337, 2009.
5. Komine, H. and Ogata, N.: Experimental study on swelling characteristics of sand-bentonite mixture for nuclear waste disposal, Soils and Foundations, Vol. 39, No. 2, pp. 83-97, 1999.
6. Komine, H. and Ogata, N.: Predicting swelling characteristics of bentonite, Journal of Geotechnical and Geoenvironmental Engineering, Vol. 130, No. 8, pp. 818-829, 2004.
7. Mitachi, T.: Mechanical behavior of bentonite-sand mixtures as buffer materials, Soils and Foundations, Vol. 48, No. 3, pp. 363-374, 2008.
8. Schanz, T., Arifin, Y.F., Khan, M.I. and Agus, S.S.: Time effects on total suction of bentonites, Soils and Foundations, Vol. 50, No. 2, pp. 195-202, 2010.
9. Ye, W.M., Borrell. N.C., Zhu, J.Y., Chen, B. and Chen, Y.B.: Advances on the investigation of the hydraulic behavior of compacted GMZ bentonite, Engineering Geology, Vol. 169, pp. 41-49, 2014.
10. Wang, Q., Tang, A.M., Cui, Y.-J., Gelage, P. and Gatmiri, B.: Experimental study on the swelling behaviour of bentonite/claystone mixture, Engineering Geology, Vol., 124, pp. 59-66, 2012.